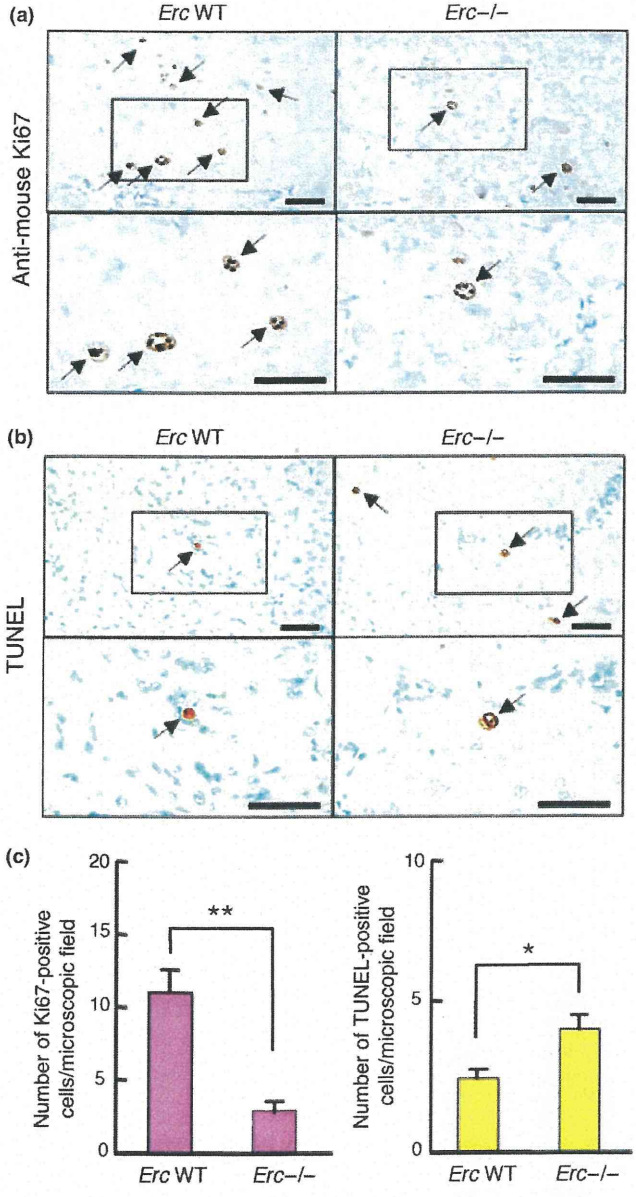

Fig. 3. Expressed in renal carcinoma (*Erc*)-deficient decreases tumor growth by impairing cell proliferation. (a) Proliferation was assessed by immunohistochemistry staining on sections of paraffin-embedded renal tumors of the indicated genotype with Ki67 antibody. Positive cells appear brown (arrows). Scale bars = 40 μm. (b) TUNEL-stained sections of paraffin-embedded renal tumors of the indicated genotype. Apoptotic cells appear brown (arrows). Scale bars = 40 μm. (c) The number of Ki67-positive cells (left panel) or TUNEL-positive cells (right panel) per microscopic field was evaluated as described in the Data S1. Values are means (n = 30 images per genotype) ± SEM; $^{**}P < 0.01$; $^{*}P < 0.05$.

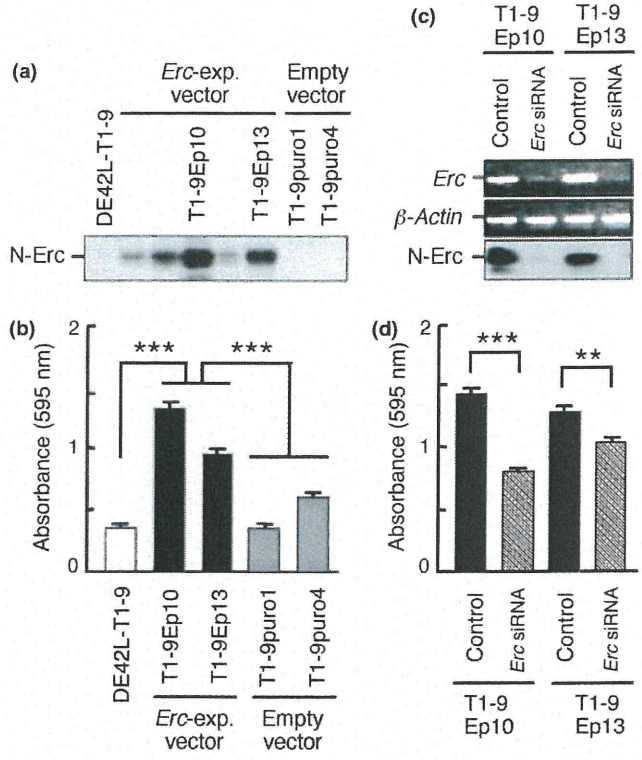

Fig. 4. Expressed in renal carcinoma (*Erc*)-expression enhanced cell adhesion to collagen-coated plates. (a) Western blot analysis showed the level of N-Erc expression in the cell lines used for cell adhesion assay. Name of each cell used for further analysis is shown. (b) The adhesion was enhanced in stable *Erc*-restored cells (T1-9Ep10 and T1-9EP13) compared with *Erc*-deficient parental cell line (DE42L-T1-9) and empty-vector cells (T1-9puro1 and T1-9puro4). Values are means ± SEM; $^{***}P < 0.001$. Three independent experiments were performed in quadruplicate. (c) RT-PCR (*Erc* and *β-Actin*) and Western blot analysis (N-Erc) showed the effects of *Erc*-suppression when treated with *Erc* siRNA in *Erc*-restored cells. (d) In contrast to results in (b), the adhesion was decreased in *Erc*-restored cells treated with siRNA. Values are means ± SEM; $^{***}P < 0.001$; $^{**}P < 0.01$. Three independent experiments were performed in quadruplicate.

DMSO (control), 10 μM Akt-I-1/2 (an Akt inhibitor) or 0.1 μM wortmannin (a phosphatidylinositol-3-OH kinase [PI3K] inhibitor), respectively, and then measured the activation of the Akt and the cell adhesion. As shown in Figure 7a, the phosphorylation of Akt (Ser473) was suppressed completely but the phosphorylation of FAK (Tyr925) was not affected in the cells that were treated with an Akt-I-1/2 or wortmannin. The cell adhesion to collagen-coated plates was remarkably decreased in *Erc*-restored cell (T1-9Ep10) treated by both inhibitors compared with control (DMSO) cells (Fig. 7b). These suggest that the activation of Akt by Erc is dependent on PI3K and the cell adhesion positively regulated by PI3K-Akt pathway because phosphorylation of FAK was not affected by Akt-inhibitor or PI3K-inhibitor treatment.

Discussion

The *Erc* gene is highly expressed in renal tumor cells compared to normal renal cells of *Tsc2*+/− KO mice. Our newly generated *Tsc2*;*Erc* double KO mice made it feasible to investigate the function of Erc in carcinogenesis in a mouse tumor model. The results clearly showed that deficiency of Erc decreased the number and size of renal tumors, and reduced cell proliferation and increased apoptosis in *Tsc2* KO mice, inhibited cell adhesion to collagen-coated plates, and suppressed tumor formation in nude mice. We also showed that Erc influenced the expression of integrin β1 and phosphorylation of several downstream proteins, such as FAK, Akt, rpS6 and Stat3.

The *Tsc2* KO mice and Eker rats, both of which are *Tsc2* heterozygous mutants, develop renal tumors through loss of *Tsc2* in

doi: 10.1111/j.1349-7006.2011.01846.x

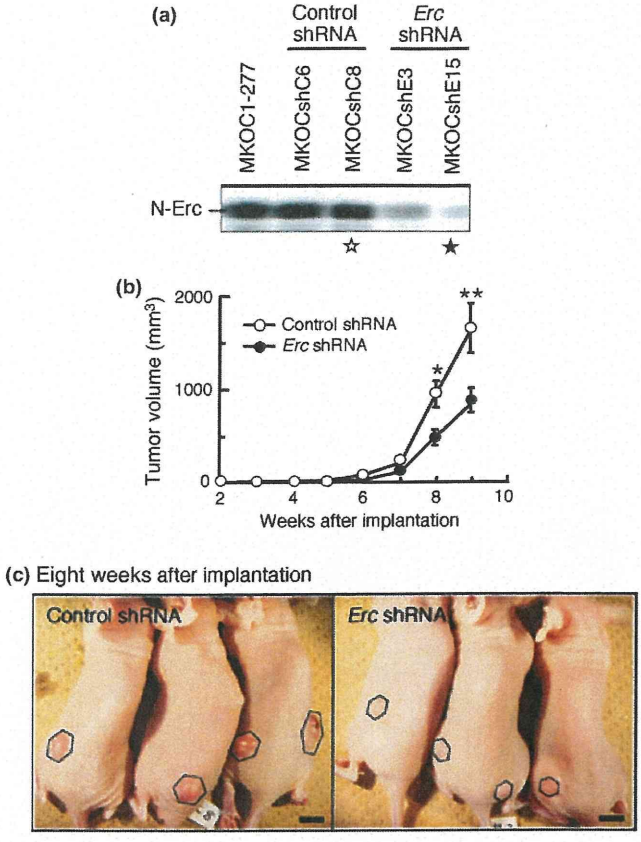

Fig. 5. Expressed in renal carcinoma (*Erc*)-deficiency suppressed tumorigenicity of renal tumor cells transplanted in nude mice. (a) Western blot analysis showed the level of N-Erc expression in the stable *Erc*-suppressed cell lines. Black and white stars indicate the cells used for tumorigenicity assay shown below. (b) The tumor volumes were suppressed in stable *Erc*-suppressed (MKOCshE15, black circles) cells compared with control-shRNA (MKOCshC8, white circles) cells after implantation into nude mice. Values are means ± SEM (n = 6); $^{**}P < 0.01$; $^{*}P < 0.05$. (c) Macroscopic appearance of tumors was shown at 8 weeks after implantation. Tumor areas are marked with hexagons. Scale bars = 10 mm.

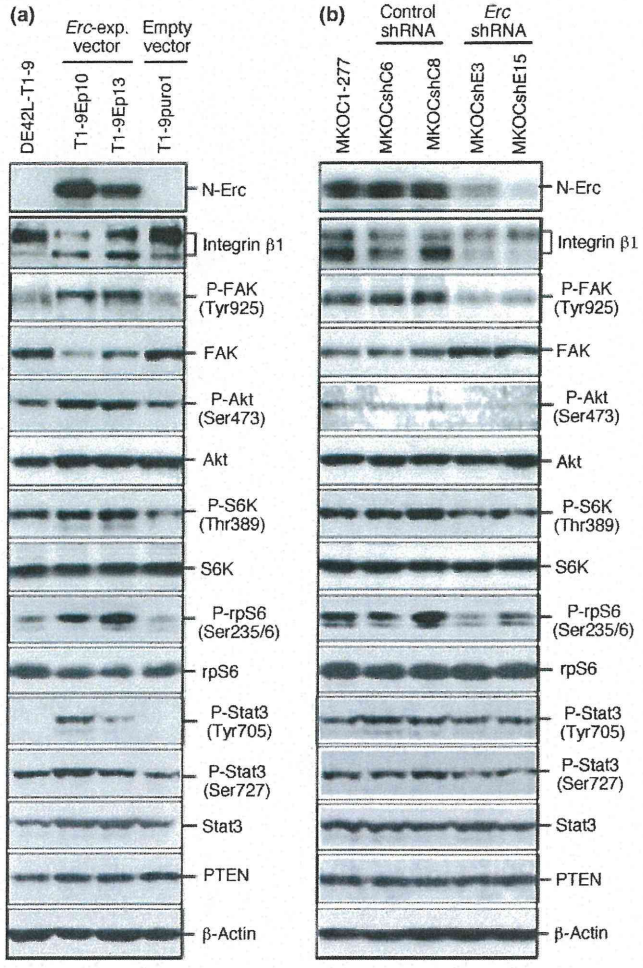

Fig. 6. Expressed in renal carcinoma (*Erc*) expression affects integrin-related signal. Western blot analysis was performed with indicated antibodies; the concentrated culture supernatant lysates were used for N-Erc and whole-cell lysates were used for other antibodies. (a) The stable *Erc*-restored cells (central two lanes) increased the precursor integrin β1 (lower-band) and the level of phosphorylation of focal adhesion kinase (FAK), Akt, S6K, rpS6 and Stat3 compared with *Erc*-deficient parental cell line (left lane) and the empty-vector cell (right lane). (b) The stable *Erc*-suppressed cells (right two lanes) decreased the precursor integrin β1 (lower-band) and the level of phosphorylation of FAK, Akt, S6K, rpS6 and Stat3 compared with *Erc*-express (WT) parental cell line (left lane) and the control-shRNA cells (central two lanes).

the WT allele and in multi-steps.[1–5] The human TSC disease is caused by germ-line mutations in either the *TSC1* or *TSC2* gene, with numerous individual tumors generally arising due to somatic ''second-hit'' mutations or loss of heterozygosity[24,40] similar to the above animal models. The resulting tumors in humans and in animal models display elevated mTOR signaling, leading to the enhanced phosphorylation of S6K and rpS6.[1–4,41,42] Erc is highly expressed in renal tumor cells of Eker rats and *Tsc2* KO mice[6,24] but the state of Erc has not been reported in human TSC disease.

The mTOR pathway has a pivotal function in the coordination of cell metabolism, cell growth and cell proliferation[40–44] but another pathway may be involved in *Tsc2* mutant animal models. It has been reported that the administration of rapamycin alone to *Tsc2*-mutant animal models (KO mice and Eker rats) with established tumors results in tumor regression. This however, is characterized with residual tumor or failure to eradicate microscopic pre-tumorous lesions.[45–47] These results suggested the existence of other pathways involved in the *Tsc2*-mutant, in addition to the mTOR axis. The *Tsc2*;*Erc* double KO mice exploited here allowed us to investigate this putative pathway without the confounding effects of possible drug resistance. Our results strongly supported the existence of another pathway, in addition to the mTOR axis.

Recently, it was reported that hotspots of GPI-anchored proteins and integrin nanoclusters were involved in cell adhesion.[48] This was corroborated by our results that showed the expression of Erc affected the pattern of integrin and phosphorylation of several kinases because Erc is one of the GPI-anchored proteins. The new pathway displaying an Erc-cell adhesion mediated tumor-proliferation function may exist, but no association between Erc and integrin-related signal has been reported. Although Erc expression is associated with the decrease in the amount of mature integrin β1, this phenomenon may be caused by some feedback mechanism from activated cell-adhesion machinery partially regulated by Erc.

Signals from the integrin complex are transmitted through the phosphorylation of FAK.[30–32] Akt is a *Tsc2*-related molecule

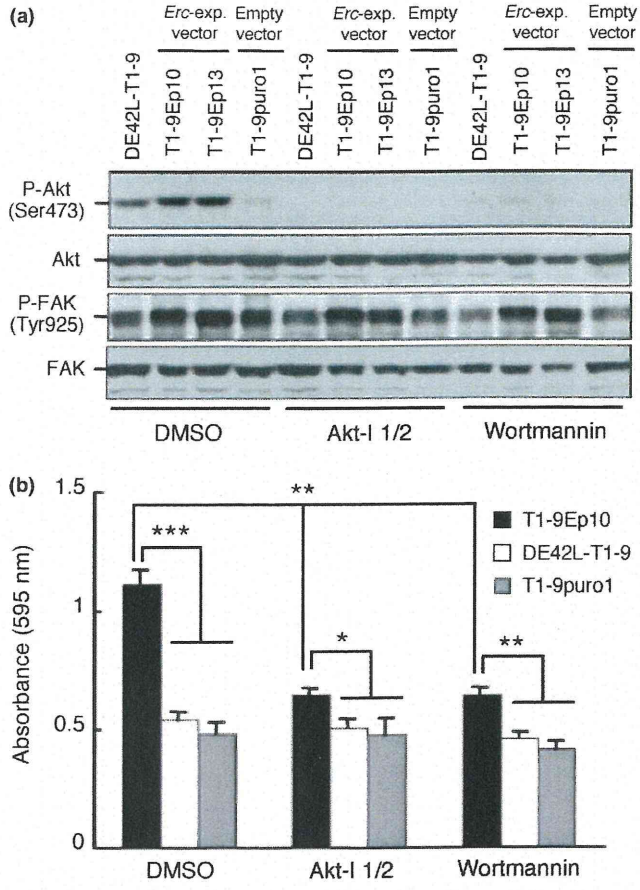

Fig. 7. Cell adhesion was decreased by treated with an Akt inhibitor and a PI3K inhibitor. The cells which are the same as Figure 6a, were divided into three groups and treated with DMSO (control), 10 μM Akt-I-1/2 (an Akt inhibitor) or 0.1 μM wortmannin (a PI3K inhibitor), respectively. (a) Western blot analysis was performed with indicated antibodies. The phosphorylation of Akt (Ser473) was suppressed completely with both the inhibitors but the phosphorylation of focal adhesion kinase (FAK; Tyr925) was not affected. (b) The cell adhesion to collagen-coated plates was remarkably decreased in *Erc*-restored cell treated by both inhibitors compared with control (DMSO) cells. Values are means ± SEM; $***P < 0.001$, $*P < 0.01$, $*P < 0.05$. Three independent experiments were performed in quadruplicate.

implicated in insulin signaling[38,39] known to be activated by cell adhesion-related signaling.[49] Our results showed that the level of phosphorylation of FAK (Tyr925), Akt (Ser473) and rpS6 (Ser235/236) were decreased with *Erc*-deficient cells (both *Erc* KO and *Erc* knock down) while the phosphorylation of S6K (Thr389) was reduced to a lesser extent, suggesting that integrin signaling and downstream proteins were upregulated by Erc.

It is well known that *Tsc2*-deficiency activates the mTORC1-S6K pathway as well as the downregulation of Akt.[50] However, our results showed the further downregulation of phosphorylation of Akt (Ser473) by *Erc*-deficiency in *Tsc2*-deficient cells and upregulation in *Erc*-restored cells *in vitro*, suggesting that *Erc*-deficiency is relevant to the suppression of tumor development in *Tsc2*+/− mice. The function of Erc might support the receptor signaling through the cell adhesion signaling. Deficiencies of *Tsc2* and *Erc* might be co-operatively involved in tumorigenesis in KO mice.

The important role of *Erc* in carcinogenesis has attracted a great deal of attention in recent years.[6–22] Several authors reported that overexpression of Erc can accelerate the proliferation and adhesion of cancer cells using cell lines and xenograft models of cancer.[9,10,17–22] Our previous study showed that *Erc* gene expression silenced by siRNA suppresses tumor growth in the *Tsc2* mutant renal carcinoma model.[51] The activation of specific signaling pathways that are important in cancer can lead to an increase in Erc expression. Binding of ovarian cancer antigen CA125/MUC16 to Erc mediates cell adhesion.[17] The overexpression of Erc in pancreatic cancer cells leads to constitutive activation of the transcription factor Stat3, which results in enhanced expression of cyclin E and cyclin E/cyclin-dependent kinase 2 complex formation, as well as increased G1-S transition.[20] Erc inhibits paclitaxel-induced apoptosis through the PI3K pathway.[21] Erc is also differentially regulated by members of the Wnt signal transduction pathway.[22] Combining these reports with our data, multiple possibilities can be considered. First, the pathological high-expression of Erc in specific malignant tumors of humans and in animal models is considered to be the result of carcinogenesis by the mutant *Tsc2* or other key gene. The pathological high-expression of Erc plays a prominent role in many signal transduction pathways such as CA125/MUC16, Stat3, PI3K and Wnt, although elucidation of the underlying mechanism remains elusive. Second, since mutant mice in which both copies of the Erc gene were inactivated showed no detectable abnormalities as compared to WT littermates,[23] Erc might have a function specific to carcinogenesis and other pathological conditions. Third, the downregulation of an integrin-related pathway may affect the progression of multi-step carcinogenesis and inhibit the development of large tumors in *Tsc2*+/−;*Erc*−/− mice.

In conclusion, we report here that deficiency of Erc affected the integrin-related signal pathway and suppressed the growth of renal tumors in *Tsc2* KO mice. An understanding of the signaling pathways and mechanisms of Erc-induced tumor cell adhesion, proliferation and survival may elucidate not only the pathogenesis of renal tumors in Tsc2+/− mice, but also the pathogenesis of other malignant tumors in both animal models and humans. Our experimental system of *Tsc*;*Erc* KO mice and cells is useful to unravel the important role of Erc during carcinogenesis, and further analysis of the Erc pathway may help to develop novel anti-cancer therapies.

Acknowledgments

We thank Nobuo Kamada, Miho Watanabe and Yousuke Kawase (Chugai Research Institute for Medical Science, Inc., Shizuoka, Japan) for mouse production; Youko Hirayama, Hiroaki Mitani, Junko Sakurai (The JFCR-Cancer Institute, Tokyo, Japan), Etsuko Kobayashi, Norihiro Tada, Fumio Kanai, Keiichi Sasahara, Naomi Ohtsuji and Tetsuya Takagaki (Juntendo University School of Medicine, Tokyo, Japan), for technical assistance; Kazunori Kajino, Shuji Momose, Shuji Matsuoka, Xianghua Piao and other members of the Hino laboratory for helpful discussions. This works was supported by a Grant-in-Aid for Cancer Research from the Ministry of Education, Science, Technology, Sports and Culture, Japan, and Grants-in-Aid for Scientific Research from Japan Society for the Promotion of Science, and the Ministry of Health, Labour and Welfare, Japan.

doi: 10.1111/j.1349-7006.2011.01846.x

References

1 Eker R, Mossige J. A dominant gene for renal adenomas in the rat. *Nature* 1961; **189**: 858–9.
2 Hino O, Kobayashi T, Momose S, Kikuchi Y, Adachi H, Okimoto K. Renal carcinogenesis: genotype, phenotype and dramatype. *Cancer Sci* 2003; **94**: 142–7.
3 Hino O, Kobayashi T, Tsuchiya H *et al.* The predisposing gene of the Eker rat inherited cancer syndrome is tightly linked to the tuberous sclerosis (TSC2) gene. *Biochem Biophys Res Commun* 1994; **203**: 1302–8.
4 Kobayashi T, Hirayama Y, Kobayashi E, Kubo Y, Hino O. A germline insertion in the tuberous sclerosis (*Tsc2*) gene gives rise to the Eker rat model of dominantly inherited cancer. *Nat Genet* 1995; **9**: 70–4.
5 Knudson AG. Mutation and cancer: statistical study of retinoblastoma. *Proc Natl Acad Sci U S A* 1971; **68**: 820–3.
6 Hino O, Kobayashi E, Nishizawa M *et al.* Renal carcinogenesis in the Eker rat. *J Cancer Res Clin Oncol* 1995; **121**: 602–5.
7 Kojima T, Oh-eda M, Hattori K *et al.* Molecular cloning and expression of megakaryocyte potentiating factor cDNA. *J Biol Chem* 1995; **270**: 21984–90.
8 Chang K, Pastan I. Molecular cloning of mesothelin, a differentiation antigen present on mesothelium, mesotheliomas, and ovarian cancers. *Proc Natl Acad Sci U S A* 1996; **93**: 136–40.
9 Yamashita Y, Yokoyama M, Kobayashi E, Takai S, Hino O. Mapping and determination of the cDNA sequence of the *Erc* gene preferentially expressed in renal cell carcinoma in the *Tsc2* gene mutant (Eker) rat model. *Biochem Biophys Res Commun* 2000; **275**: 134–40.
10 Hassan R, Bera T, Pastan I. Mesothelin: a new target for immunotherapy. *Clin Cancer Res* 2004; **10**: 3937–42.
11 Scholler N, Fu N, Yang Y *et al.* Soluble member(s) of the mesothelin/megakaryocyte potentiating factor family are detectable in sera from patients with ovarian carcinoma. *Proc Natl Acad Sci U S A* 1999; **96**: 11531–6.
12 Sapede C, Gauvrit A, Barbieux I *et al.* Aberrant splicing and protease involvement in mesothelin release from epithelioid mesothelioma cells. *Cancer Sci* 2008; **99**: 590–4.
13 Li M, Bharadwaj U, Zhang R *et al.* Mesothelin is a malignant factor and therapeutic vaccine target for pancreatic cancer. *Mol Cancer Ther* 2008; **7**: 286–96.
14 Robinson BW, Creaney J, Lake R *et al.* Mesothelin-family proteins and diagnosis of mesothelioma. *Lancet* 2003; **362**: 1612–6.
15 Hino O, Maeda M. Diagnostic tumor marker of asbestos-related mesothelioma. *Environ Health Prev Med* 2008; **13**: 71–4.
16 Shiomi K, Hagiwara Y, Sonoue K *et al.* Sensitive and specific new enzyme-linked immunosorbent assay for N-ERC/mesothelin increases its potential as a useful serum tumor marker for mesothelioma. *Clin Cancer Res* 2008; **14**: 1431–7.
17 Rump A, Morikawa Y, Tanaka M *et al.* Binding of ovarian cancer antigen CA125/MUC16 to mesothelin mediates cell adhesion. *J Biol Chem* 2004; **279**: 9190–8.
18 Hucl T, Brody JR, Gallmeier E, Iacobuzio-Donahue CA, Farrance IK, Kern SE. High cancer-specific expression of mesothelin (MSLN) is attributable to an upstream enhancer containing a transcription enhancer factor dependent MCAT motif. *Cancer Res* 2007; **67**: 9055–65.
19 Que J, Wilm B, Hasegawa H, Wang F, Bader D, Hogan BL. Mesothelium contributes to vascular smooth muscle and mesenchyme during lung development. *Proc Natl Acad Sci U S A* 2008; **105**: 16626–30.
20 Bharadwaj U, Li M, Chen C, Yao Q. Mesothelin-induced pancreatic cancer cell proliferation involves alteration of cyclin E via activation of signal transducer and activator of transcription protein 3. *Mol Cancer Res* 2008; **6**: 1755–65.
21 Chang MC, Chen CA, Hsieh CY *et al.* Mesothelin inhibits paclitaxel-induced apoptosis through the PI3K pathway. *Biochem J* 2009; **424**: 449–58.
22 Prieve MG, Moon RT. Stromelysin-1 and mesothelin are differentially regulated by Wnt-5a and Wnt-1 in C57MG mouse mammary epithelial cells. *BMC Dev Biol* 2003; **3**: 2–11.
23 Bera TK, Pastan I. Mesothelin is not required for normal mouse development or reproduction. *Mol Cell Biol* 2000; **20**: 2902–6.
24 Kobayashi T, Minowa O, Kuno J, Mitani H, Hino O, Noda T. Renal carcinogenesis, hepatic hemangiomatosis, and embryonic lethality caused by a germ-line *Tsc2* mutation in mice. *Cancer Res* 1999; **59**: 1206–11.
25 Gustavsson A, Armulik A, Brakebusch C, Fässler R, Johansson S, Fällman M. Role of the β1-integrin cytoplasmic tail in mediating invasin-promoted internalization of Yersinia. *J Cell Sci* 2002; **115**: 2669–78.
26 Harburger DS, Calderwood DA. Integrin signalling at a glance. *J Cell Sci* 2009; **122**: 159–63.
27 Macias-Perez I, Borza C, Chen X *et al.* Loss of integrin α1 β1 ameliorates Kras-induced lung cancer. *Cancer Res* 2008; **68**: 6127–35.
28 Brenner W, Greber I, Gudejko-Thiel J *et al.* Migration of renal carcinoma cells is dependent on protein kinase Cdelta via beta1 integrin and focal adhesion kinase. *Int J Oncol* 2008; **32**: 1125–31.
29 Park CC, Zhang H, Pallavicini M *et al.* Beta1 integrin inhibitory antibody induces apoptosis of breast cancer cells, inhibits growth, and distinguishes malignant from normal phenotype in three dimensional cultures and in vivo. *Cancer Res* 2006; **66**: 1526–35.
30 Shibue T, Weinberg RA. Integrin β1-focal adhesion kinase signaling directs the proliferation of metastatic cancer cells disseminated in the lungs. *Proc Natl Acad Sci U S A* 2009; **106**: 10290–5.
31 Xia H, Nho RS, Kahm J, Kleidon J, Henke CA. Focal adhesion kinase is upstream of phosphatidylinositol 3-kinase/Akt in regulating fibroblast survival in response to contraction of type I collagen matrices via a beta 1 integrin viability signaling pathway. *J Biol Chem* 2004; **279**: 33024–34.
32 Pylayeva Y, Gillen KM, Gerald W, Beggs HE, Reichardt LF, Giancotti FG. Ras- and PI3K-dependent breast tumorigenesis in mice and humans requires focal adhesion kinase signaling. *J Clin Invest* 2009; **119**: 252–66.
33 Argraves WS, Suzuki S, Arai H, Thompson K, Pierschbacher MD, Ruoslahti E. Amino acid sequence of the human fibronectin receptor. *J Cell Biol* 1987; **105**: 1183–90.
34 Guo HB, Lee I, Kamar M, Akiyama SK, Pierce M. Aberrant *N*-glycosylation of beta1 integrin causes reduced alpha5beta1 integrin clustering and stimulates cell migration. *Cancer Res* 2002; **62**: 6837–45.
35 Bellis SL, Newman E, Friedman EA. Steps in integrin beta1-chain glycosylation mediated by TGFbeta1 signaling through Ras. *J Cell Physiol* 1999; **181**: 33–44.
36 Isaji T, Sato Y, Fukuda T, Gu J. *N*-glycosylation of the I-like domain of beta1 integrin is essential for beta1 integrin expression and biological function: identification of the minimal *N*-glycosylation requirement for alpha5beta1. *J Biol Chem* 2009; **284**: 12207–16.
37 Bellis SL. Variant glycosylation: an underappreciated regulatory mechanism for beta1 integrins. *Biochim Biophys Acta* 2004; **1663**: 52–60. Review.
38 Inoki K, Corradetti MN, Guan KL. Dysregulation of the TSC-mTOR pathway in human disease. *Nat Genet* 2005; **37**: 19–24.
39 Cao Y, Kamioka Y, Yokoi N *et al.* Interaction of FoxO1 and TSC2 induces insulin resistance through activation of the mammalian target of rapamycin/p70 S6K pathway. *J Biol Chem* 2006; **281**: 40242–51.
40 Astrinidis A, Henske EP. Tuberous sclerosis complex: linking growth and energy signaling pathways with human disease. *Oncogene* 2005; **24**: 7475–81.
41 Kobayashi T, Adachi H, Mitani H, Hirayama Y, Hino O. Toward chemotherapy for *Tsc2 mutant* renal tumor. *Proc Jpn Acad* 2003; **79**: 22–5.
42 Shiono M, Kobayashi T, Takahashi R *et al.* The G1556S-type tuberin variant suppresses tumor formation in tuberous sclerosis 2 mutant (Eker) rats despite its deficiency in mTOR inhibition. *Oncogene* 2008; **27**: 6690–7.
43 Guertin DA, Sabatini DM. Defining the role of mTOR in cancer. *Cancer Cell* 2007; **12**: 9–22.
44 Gan B, Yoo Y, Guan J-L. Association of focal adhesion kinase with tuberous sclerosis complex 2 in the regulation of s6 kinase activation and cell growth. *J Biol Chem* 2006; **281**: 37321–9.
45 Kenerson H, Dundon TA, Yeung RS. Effects of rapamycin in the Eker rat model of tuberous sclerosis complex. *Pediatr Res* 2005; **57**: 67–75.
46 Lee L, Sudentas P, Donohue B *et al.* Efficacy of a rapamycin analog (CCI-779) and IFN-gamma in tuberous sclerosis mouse models. *Genes Chromosomes Cancer* 2005; **42**: 213–27.
47 Lee L, Sudentas P, Dabora SL. Combination of a rapamycin analog (CCI-779) and interferon-gamma is more effective than single agents in treating a mouse model of tuberous sclerosis complex. *Genes Chromosomes Cancer* 2006; **45**: 933–44.
48 van Zanten TS, Cambi A, Koopman M *et al.* Hotspots of GPI-anchored proteins and integrin nanoclusters function as nucleation sites for cell adhesion. *Proc Natl Acad Sci U S A* 2009; **106**: 18557–62.
49 Barros CS, Nguyen T, Spencer KS, Nishiyama A, Colognato H, Müller U. β1 integrins are required for normal CNS myelination and promote AKT-dependent myelin outgrowth. *Development* 2009; **136**: 2717–24.
50 Huang J, Wu S, Wu CL, Manning BD. Signaling events downstream of mammalian target of rapamycin complex 2 are attenuated in cells and tumors deficient for the tuberous sclerosis complex tumor suppressors. *Cancer Res* 2009; **69**: 6107–14.
51 Imamura O, Okada H, Takashima Y, Zhang D, Kobayashi T, Hino O. siRNA-mediated Erc gene silencing suppresses tumor growth in Tsc2 mutant renal carcinoma model. *Cancer Lett* 2008; **268**: 278–85.

Supporting Information

Additional Supporting Information may be found in the online version of this article:

Data S1. Supporting Methods.

Fig. S1. Establishment of expressed in renal carcinoma (*Erc*) KO mice.

Fig. S2. Amino acid alignment of the expressed in renal carcinoma (Erc)/mesothelin protein.

Fig. S3. Enhanced tumorigenicity of expressed in renal carcinoma (*Erc*)-restored renal tumor cells transplanted in nude mice.

Fig. S4. Confirmed the characteristics of integrin β1 by treated with lower concentration of tunicamycin.

doi: 10.1111/j.1349-7006.2011.01846.x

The Journal of Toxicological Sciences (J. Toxicol. Sci.)
Vol.35, No.4, 437-446, 2010

Original Article

Effects of preparation methods for multi-wall carbon nanotube (MWCNT) suspensions on MWCNT induced rat pulmonary toxicity

Kiyoshi Wako[1], Yuri Kotani[1], Akihiko Hirose[2], Takuya Doi[1] and Shuichi Hamada[1]

[1]Kashima Laboratory, Mitsubishi Chemical Medience Corporation, 14 Sunayama, Kamisu-shi, Ibaraki 314-0255, Japan
[2]Division of Risk Assessment, Biological Safety Research Center, National Institute of Health Sciences, 1-18-1 Kamiyoga, Setagaya-ku, Tokyo 158-8501, Japan

(Received October 27, 2009; Accepted February 24, 2010)

ABSTRACT — Since there is a possibility of inhaling the fibers of multi-wall carbon nanotube (MWCNT) without any agglomeration, it is important that the pulmonary toxicity is evaluated by intratracheal instillation without agglomeration. MWCNT suspended in an artificial lung surfactant (ALS) with or without grinding in an agate mortar was instilled once intratracheally to rats to determine whether differences of the effects to pulmonary toxicity by different amounts of agglomerated MWCNT particle. The MWCNT suspension preparation method with grinding was effective at reducing agglomerates and in increasing uniform dispersion of the fibers. The ground MWCNT induced higher LDH levels and neutrophil ratios in the bronchoalveolar lavage fluid (BALF). There were no remarkable responses in rats in the non-ground MWCNT group, with the exception of inflammatory responses in the early phase. Some histopathological findings varied between rats given the ground MWCNT and non-ground MWCNT. A major difference was an MWCNT-laden macrophage infiltration site in the lung, which were in the alveolus in the ground MWCNT group, and in the interstitium in non-ground MWCNT group. Accordingly, the preparation method with grinding is considered to be effective at reducing agglomerates and ensuring uniform dispersion of the fibers. These findings lead us to conclude that the amount of agglomerates in the suspension is an important factor affecting the pulmonary toxicity of MWCNT.

Key words: Multi-wall carbon nanotube (MWCNT), Rats, Lung toxicity, Inflammation

INTRODUCTION

The production of multi-wall carbon nanotube (MWCNT), a representative industrial nanomaterial, is increasing worldwide due to their high potentials in industrial usage. Recent reports (Lam *et al.*, 2006; Donaldson *et al.*, 2006) suggested that the health effects of such materials must be evaluated properly. It is estimated that a possible exposure route of MWCNT is inhalation, especially in occupational environments. The shape of MWCNT is similar to asbestos and has been reported to induce mesothelioma like lesions (Takagi *et al.*, 2008; Poland *et al.*, 2008). Therefore, assessment of pulmonary toxicity of MWCNT with experimental animals is important to ascertain the possible effects on human health. The first evaluation of MWCNT inducing pulmonary toxicity was made by an intratracheal instillation with rodents. However, the information regarding MWCNT induced pulmonary toxicity in rodents is limited (Muller *et al.*, 2005).

It is well known that MWCNT tends to agglomerate into large particles, such as in the micrometer-order scale (Lam *et al.*, 2006). Studies in which large particulate of MWCNT are intratracheally administered and evaluated may lead to a misunderstanding of its pulmonary toxicity. Therefore, the preparation method of finely dispersing MWCNT is essential to assess its pulmonary toxicity.

The present study examined the preparation methods of MWCNT suspensions for intratracheally instilling finely dispersed fibers as well as the effects of different dispersion conditions of MWCNT fibers in suspensions on pulmonary toxicity in rats.

Correspondence: Kiyoshi Wako (E-mail: Wako.Kiyoshi@mv.medience.co.jp)

MATERIALS AND METHODS

Experimental animals

Female Crl:CD(SD) rats with a body weight range of 170 to 200 g were obtained from Charles River Laboratories Japan, Inc. (Kanagawa, Japan). The animals were kept in an animal room of the Kashima Laboratory, Mitsubishi Chemical Medience Corporation (Ibaraki, Japan), which was maintained at temperature of 22 ± 2°C, relative humidity of 55 ± 20%, with a 12 hr light-dark cycle. They were given tap water and a diet for experimental animals (MF: Oriental Yeast Co., Ltd., Tokyo, Japan) *ad libitum*. The rats were 8 weeks old at dosing. The present study was carried out in accordance with the Guidelines for Animal Studies (Toxicological Science Division, Mitsubishi Chemical Medience Corporation). Moreover, the protocol of this study was approved by the Committee for Ethics in Animal Studies of the Kashima Laboratory prior to commencing the study.

Materials

MWCNT (MITSUI MWCNT-7, Lot No. 060125-01k) and crystalline silica (Min-U-Sil #5: provided by Hayashi-Kasei Co., Ltd., Osaka, Japan) were used in this study. The property of the MWCNT is the same as those formerly reported (Takagi *et al.*, 2008). Briefly, MWCNT has a density of 3.55×10^{11} particles/g. The length and width were examined with a scanning electron microscope and are indicated in Fig. 1. MWCNT contained; Fe (approximately 3,500 ppm), sulfur (470 ppm), and chlorine (20 ppm) as well as fluorine (5 ppm) and bromide (40 ppm) that were below the detection levels.

Preparation of particle suspension

There were large numbers of agglomerates in suspensions prepared using media such as, 0.5% CMC-Na solution, 0.1% Tween 80 solution, or 0.5% CMC-Na solution containing 0.1% Tween 80. In contrast, the numbers of agglomerates decreased when an artificial lung surfactant (ALS, Surfacten®: Mitsubishi Tanabe Pharma Corp., Osaka, Japan) was used as the suspension media. Therefore, the ALS was selected as the suspension media for this study. Surfacten® is an extraction from bovine lung, which include a constant ratio of phospholipids, free fatty acids, and triglyceride. ALS was prepared by dissolving Surfacten® at 120 mg into sterilized saline (Otsuka Normal Saline: Otsuka Pharmaceutical Factory, Inc., Tokushima, Japan) at 4 ml. MWCNT was suspended in ALS at a concentration of 10 mg/ml with or without grinding in an agate mortar, the suspension was subjected to sonication for 3 min with an ultrasonic disruptor (UD-201: Tomy Seiko Co., Ltd., Tokyo, Japan). The grinding was conducted under wet conditions: ground after addition of a small amount of ALS to an adequate amount of MWCNT, and filled up to the proper volume with ALS to make target concentrations. The dispersion conditions were evaluated with a light microscope, transmission electron microscope (H-7600: Hitachi, Tokyo, Japan), and scanning electron microscope (JSM-5200: JEOL, Tokyo, Japan).

Min-U-Sil #5 was also suspended in ALS at a concentration of 10 mg/ml, and sonicated for 3 min.

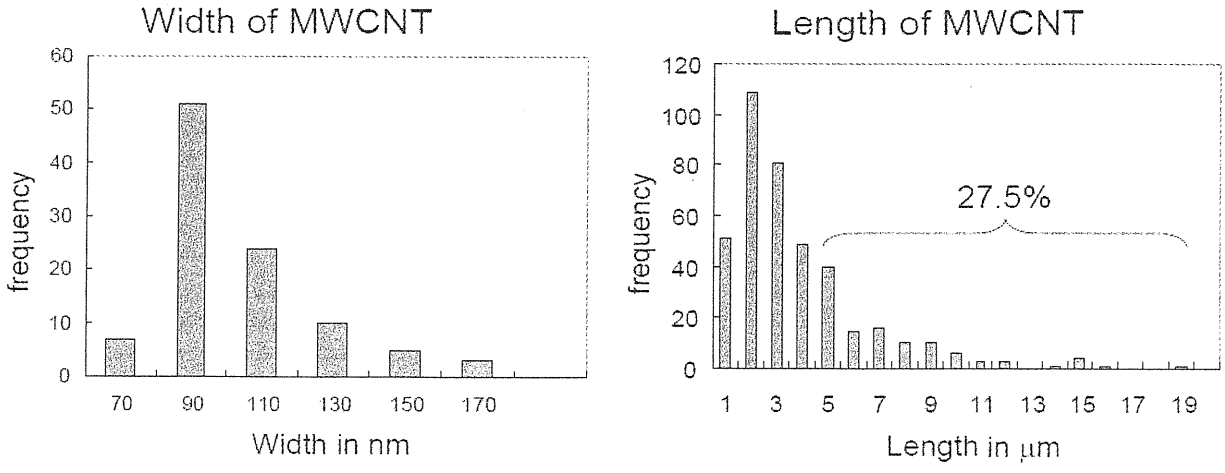

Fig. 1. Width and length distribution of MWCNT: The average width was about 100 nm, and 27.5% of the particles were longer than 5 μm.

Particle instillation

The light anesthetization was achieved by ether inhalation. An 18-G intravenous catheter (Terumo Corp., Tokyo, Japan) was inserted to the larynx as a guide to insert a narrow catheter. The suspensions (volume: 0.5 ml/animal) were instilled to the trachea via the narrow catheter (outside diameter: 0.80 mm).

General experimental design

The suspensions of the ground MWCNT, non-ground MWCNT, Min-U-Sil, and ALS alone (as a negative control) were administered intratracheally at a dose of 5 mg/animal with a dosage volume of 0.5 ml/animal to 12 rats/group. Since it was reported that the dose at 5 mg/head of MWCNT had toxicological effects on the lung according to Muller *et al.* (2005), this dose was selected for this study. Furthermore, this dosage volume is widely used in similar studies. The day of administration was designated as Day 1. Three rats from each group were subjected to necropsy on Days 2, 8, 29, and 92 after peritoneal injection of pentobarbital sodium (Nembutal®: Dainippon Sumitomo Pharma Co., Ltd., Osaka, Japan). Bronchoalveolar lavage fluid (BALF) was obtained from all rats on each day of necropsy. The difference in the effects on pulmonary toxicity by the amount of agglomerated particles in the instilled suspension was assessed by BALF analysis and histological examination.

BALF analysis

Firstly, the right lung lobes after ligating of the left bronchus were lavaged three times with 3 ml of saline (Otsuka Normal Saline: Otsuka Pharmaceutical Factory Inc.) heated up to 37°C in advance for the cell-counting procedure. A cell pellet was obtained from the BALF after centrifugation (300 × g, 10 min) at about 4°C. The cell pellet was re-suspended in 0.1% BSA containing phosphate buffered saline (PBS^-) + 0.05 mM EDTA-2K and cell count and deferential ratio were examined with a hemocytometer (XT-2000iV: Sysmex Corp., Hyogo, Japan). Secondary, the right lung lobes were lavaged once with 2 ml of saline. The obtained BALF was mixed with the previously obtained supernatant and centrifuged (300 × g, 10 min) at about 4°C. The supernatant thus obtained was subjected to the quantification of protein (Biuret method) and LDH (UV-rate method, JSCC modified method) with an automatic analyzer (TBA-200FR: Toshiba Corp., Tokyo, Japan).

Histological examination

The left lung lobes and bronchiolar lymph nodes were removed and fixed in 10% phosphate-buffered formalin. After conventional processing, paraffin-embedded sections were stained with hematoxylin and eosin (H&E) and examined histopathologically under a light microscope. Moreover, a part of the lung was collected from one animal of each group and fixed in 2.5% glutaraldehyde with negative pressure. The lungs were embedded in epoxy resin and stained with uranyl acetate and lead citrate for examination with a transmission electron microscope (H-7600: Hitachi).

Statistical analysis

The cell differential ratio as well as protein and LDH concentrations in BALF were statistically compared with the control values for each time point. Initially, the variance was assessed with Bartlett's test. When the variance was equal, one-way analysis of variance was used; otherwise, the Kruskal-Wallis test was used. When significant differences were seen between the groups, they were evaluated with Dunnett's method (homogeneous variance) or a Dunnett's type (Steel method; non-homogeneous variance) multiple comparison test. The significance was judged at the 0.01 and 0.05 probability levels. Additionally, the above values were examined between the non-ground MWCNT and ground MWCNT groups. Initially, the variance was assessed with the F test with a significant level of 5%. Significant differences between the groups were then analyzed using the Student's t test when the variance was equal; otherwise, the Aspin-Welch's test was used.

RESULTS

Grinding effects

The effects of grinding with an agate mortar were evaluated by observation of the suspensions with a light microscope and electron microscope (Figs. 2, 3, and 4). The agglomerates in the ground MWCNT were smaller than those in the non-ground MWCNT. The number of fibers finely dispersed was observed in the ground MWCNT. The length of the fiber in the ground MWCNT was smaller than those in the non-ground MWCNT.

BALF analysis

The following results were obtained as compared to the control values. The total cell count in BALF elevated in rats given the ground MWCNT on Day 8 and Min-U-Sil on Day 91. Higher neutrophil ratios in BALF were observed in rats given the non-ground MWCNT and ground MWCNT on Day 2, ground MWCNT and Min-U-Sil on Day 29, and Min-U-Sil on Day 91 (Fig. 5). Higher LDH concentrations in BALF were observed in rats given

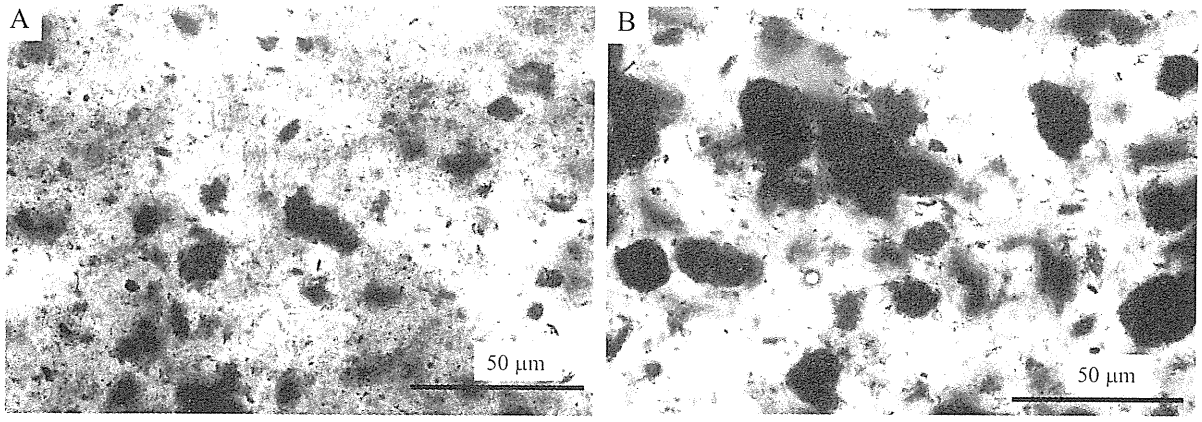

Fig. 2. Light microscopic view of administered MWCNT suspension: A) Ground MWCNT suspension, sizes of agglomerates were smaller than non-ground MWCNT suspension and finely dispersed fibers were seen. B) Non-ground MWCNT suspension, large agglomerates and small number of dispersed fibers were seen. Original magnifications were x 400.

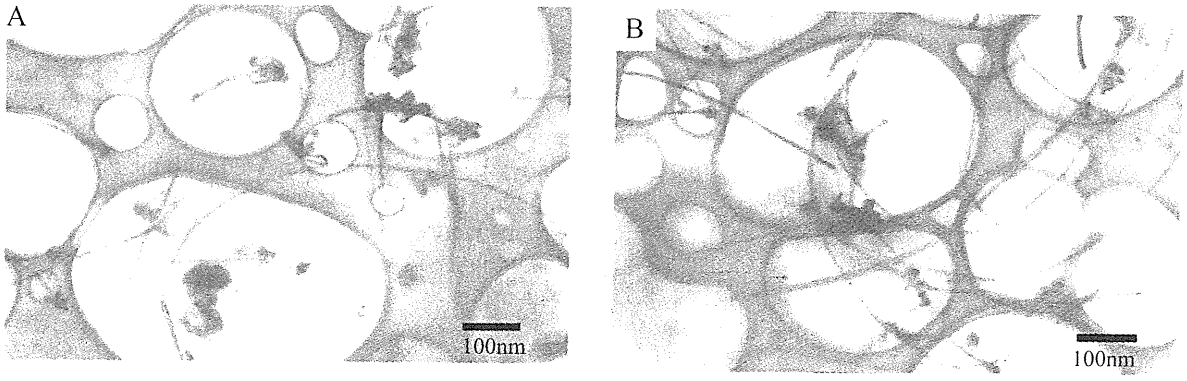

Fig. 3. Transmission electron microscopic view of administered MWCNT suspension: A) Ground MWCNT suspension, short fibers were seen. B) Non-ground MWCNT suspension, long fibers were seen.

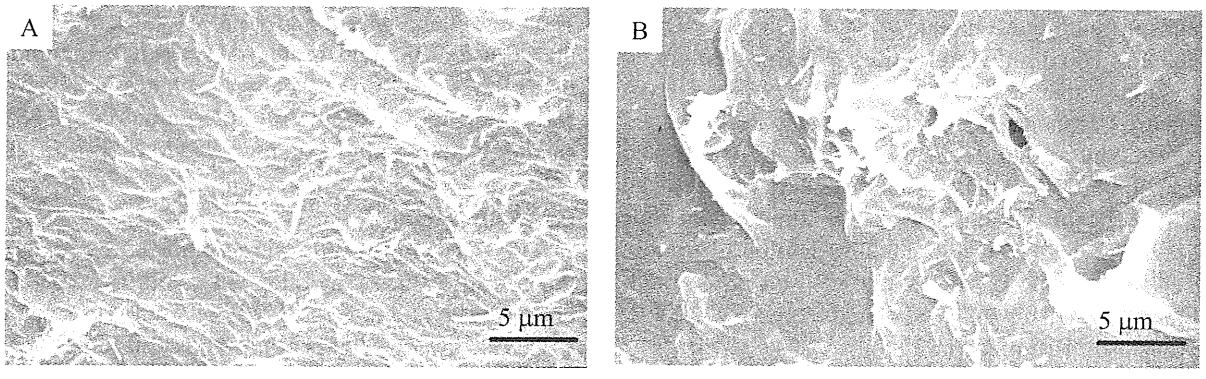

Fig. 4. Scanning electron microscopic view of administered MWCNT suspension: A) Ground MWCNT suspension, uniform suspended condition was seen with small size of fibers. B) Non-ground MWCNT suspension, non-uniform suspended condition and agglomerates were seen.

the non-ground MWCNT and ground MWCNT on Day 8, ground MWCNT and Min-U-Sil on Day 29, as well as Min-U-Sil on Day 91. Higher protein levels in BALF were observed in all treated rats on Day 91 (Fig. 6). There were no remarkable differences in these parameters between rats given the non-ground and ground MWCNT.

Histological examination

Tables 1 and 2 summarized histopathological findings. Black patches in the lung and blackish change of the bronchiolar lymph nodes were macroscopically observed in rats given the non-ground and ground MWCNT. MWCNT, which was "blackish" in color, and was microscopically observed in the alveolar region of rats given the ground MWCNT on Day 2. In rats given the non-ground MWCNT, MWCNT was slightly observed in the bronchial region. On Day 8 or later, focal infiltration of MWCNT- laden macrophages were observed in the interstitium of the lung of rats given the non-ground MCNT, compared to rats given the ground MWCNT, where macrophages were observed mainly in the alveolus. Ultrastructurally, the macrophages in the alveolus of rats given the ground MWCNT had well-developed lysosomes (Figs. 7 and 9). In the bronchiolar lymph nodes of rats given the non-ground and ground MWCNT, there were black colored macrophage infiltrations, which were thought to be phagocytosed MWCNT. The severity of the black colored macrophage infiltrations in the bronchiolar lymph nodes progressively increased after Day 29 in rats given the ground MWCNT (Fig. 8). Focal inflammatory cell infiltration in the lungs was observed in rats given the non-ground and ground MWCNT on Day 2 only, however, it was observed in rats given Min-U-Sil not only on Day 2 but also on Day 92. In rats given Min-U-Sil, granuloma in the bronchiolar lymph nodes was observed on Day 92.

DISCUSSION

This study led to a conclusion that the ALS is one of the most suitable vehicle media to suspend MWCNT for intratracheal instillation. Buford *et al.* (2007) reported that the vehicle containing some protein, lipid or protein/

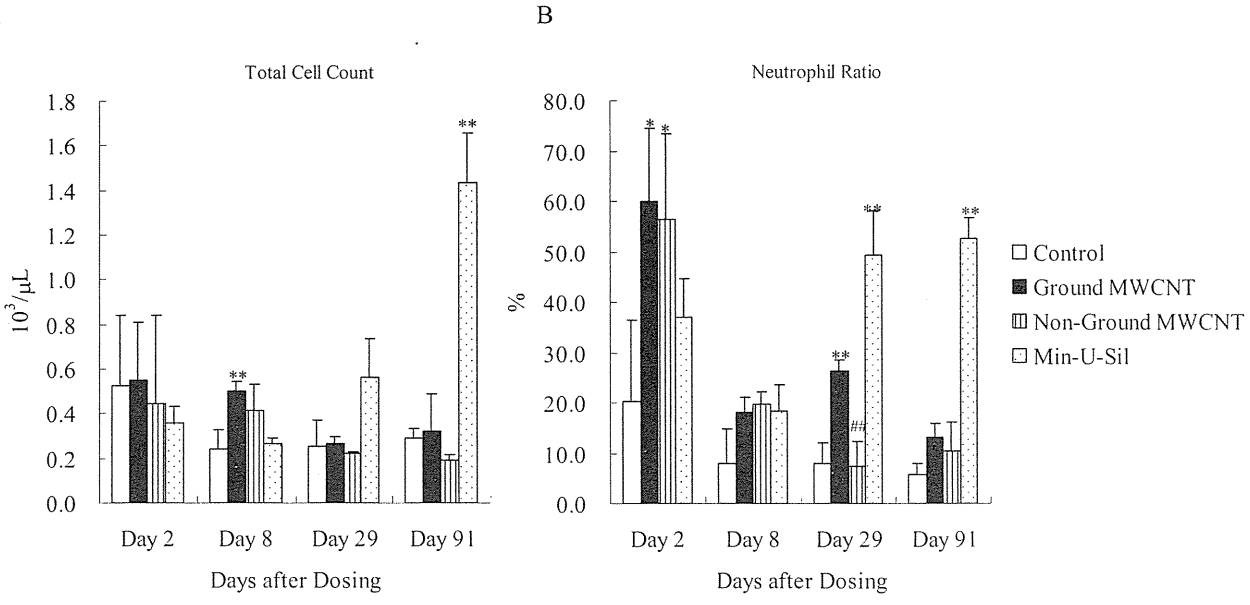

Fig. 5. A) Total cell count in broncho-alveolar lavage fluids (BALF) from rats exposed to non-ground and ground MWCNT, and corresponding controls on days 2, 8, 29, and 91 (day of dosing designated as day 1). Values are mean ± S.D. Ground MWCNT induced significantly increasing of total cell count in BALF on day 8, $^{**}p < 0.01$. Min-U-Sil induced significantly increasing of total cell count in BALF on day 91, $^{**}p < 0.01$.
B) Neutrophil ratio in BALF from rats exposed to ground, non-ground MWCNT and corresponding controls on days 2, 8, 29, and 91. Values are mean ± S.D. Ground and non-ground MWCNT induced higher neutrophil ratio in BALF on days 2, $^{*}p < 0.05$, and ground MWCNT induced the higher neutrophil ratio on day 29, $^{**}p < 0.01$. Neutrophil ratio in non-ground MWCNT on day 29 significantly lower than ground MWCNT, $^{\#\#}p < 0.05$. Min-U-Sil induced higher neutrophil ratio on days 29 and 91, $^{*}p < 0.01$.

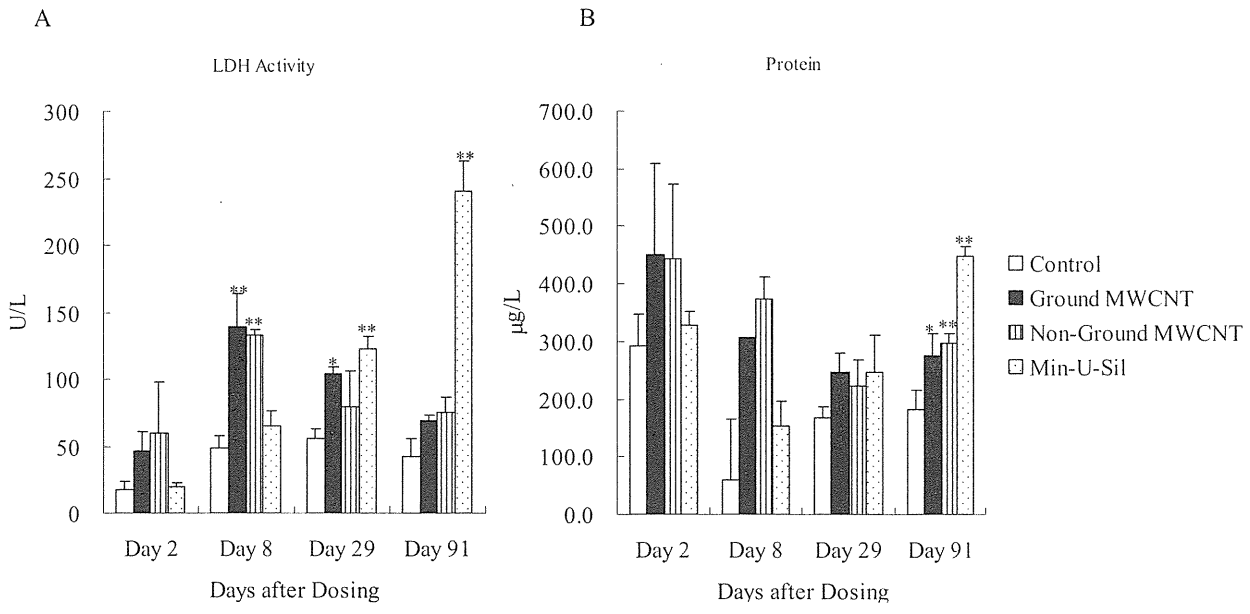

Fig. 6. A) LDH activity in BALF from rats exposed to non-ground and ground MWCNT, and corresponding controls on days 2, 8, 29, and 91 (day of dosing designated as day 1). Values are mean ± S.D. Ground MWCNT induced significantly increasing of LDH activity on days 8 and 29, non-ground MWCNT induced higher LDH activity on day 8 only, $*p < 0.05$ and $**p < 0.01$. Min-U-Sil induced higher LDH activity on days 29 and 91, $**p < 0.01$.
B) Total protein concentration in BALF from rats exposed to ground, non-ground MWCNT and corresponding controls on days 2, 8, 29, and 91. Values are mean ± S.D. Ground and non-ground MWCNT, and Min-U-Sil induced higher protein level in BALF on day 91, $*p < 0.05$ and $**p < 0.01$.

lipid component could disperse carbon nanotubes appropriately. Since the ALS used in this study is an extraction from bovine lung, which includes phospholipids, free fatty acids, and triglyceride, the results of this study did not contradict their report (Buford *et al.*, 2007). Additionally, although no remarkable adverse effects were noted by dosing of the xenogeneic media, the possible pulmonary toxicity of MWCNT may have to be evaluated by removing the influence of the xenogeneic agent. It is considered that the suspension preparation method recently reported (Buford *et al.*, 2007; Sager *et al.*, 2007) is suitable for this purpose.

The results of this study suggested that the wet-grinding in an agate mortar was useful to prepare uniform dispersed suspension, because it was confirmed that the grinding reduced the number and the size of the agglomerates in the suspensions. Since grinding with a mortar is a simple procedure, it was concluded that this method is appropriate for preparation of any other CNT suspensions for intratracheal instillation. Furthermore, this method reduced generation of MWCNT aerosol when conducted under wet conditions. This suggested that the possibility of inhalation of aerosolized MWCNT to human could be reduced with this method.

There were remarkable differences between the ground MWCNT and non-ground MWCNT in the BALF chemistry analysis on Day 29. Higher neutrophil ratios and LDH levels in the BALF were observed in rats given the ground MWCNT on Day 29. In contrast, such changes were not noted in rats given the non-ground MWCNT. There were remarkable differences in histological changes of the lungs between rats given the ground and non-ground MWCNT. In rats given the ground MWCNT, remarkable macrophage infiltration in the alveolus was observed, but in the interstitium it was relatively weak. In contrast, there was predominant macrophage infiltration in the interstitium of rats given the non-ground MWCNT.

Muller *et al.* (2005) reported that ground MWCNT led the pulmonary lesion characterized by the interstitial fibrosis in the lungs. MWCNT-laden macrophage infiltration in the alveolus was considered to be attributable to the relatively short fiber, which was generated by grinding. The acceleration of phagocytic activity, which was demonstrated as an increase of developed lysosomes supported our speculation.

There were no inflammatory responses in the bronchi-

Table 1. Numbers of rats indicating the histopathological lesions in the bronchiolar lymph node and trachea of rats given ground or non-ground multiwall carbon nanotube, Min-U-Sil, or artificial lung surfactant

Organ			Group name															
Findings			Control				Ground MWCNT				Non-Ground MWCNT				Min-U-Sil			
	Grade	Day:	2	8	29	92	2	8	29	92	2	8	29	92	2	8	29	92
Lymph node, bronchial																		
Cell infiltration, macrophage	1		0	0	0	0	0	3	0	0	0	0	3	1	0	0	0	0
	2		0	0	0	0	0	0	3	3	0	0	0	1	0	0	0	0
Granuloma	1		0	0	0	0	0	0	0	0	0	0	0	0	0	0	1	0
	2		0	0	0	0	0	0	0	0	0	0	0	0	0	0	2	0
	3		0	0	0	0	0	0	0	0	0	0	0	0	0	0	0	3
Trachea																		
Accumulation, administered substance	1		0	0	0	0	3	0	0	0	2	0	0	0	0	0	0	0
Cell infiltration, inflammatory, mucosa	1		0	0	0	0	1	0	0	0	0	0	0	0	2	0	0	0
Regeneration, mucosa, focal	1		1	0	0	0	2	0	0	0	1	0	0	0	0	0	0	0
Ulcer	1		0	0	0	0	3	0	0	0	1	0	0	0	0	0	0	0
	2		0	0	0	0	0	0	0	0	0	0	0	0	0	0	0	0
	3		0	0	0	0	0	0	0	0	1	0	0	0	0	0	0	0
Hypertrophy, mucosal epithelium	1		0	0	0	0	0	1	0	0	0	1	0	0	0	0	0	0
Cell infiltration, macrophage, lamina propria, focal	1		0	0	0	0	0	0	0	0	0	0	1	0	0	0	1	0

Note: values indicate number of animals indicating lesion.
Grade: 1 = minimal, 2 = mild, 3 = moderate. Day: day of intratracheal instillation designated as Day 1.

Table 2. Numbers of rats indicating the histopathological lesions in the lung of rats given ground or non-ground multiwall carbon nanotube, Min-U-Sil, or artificial lung surfactant

Organ			Group name															
Findings			Control				Ground MWCNT				Non-Ground MWCNT				Min-U-Sil			
	Grade	Day:	2	8	29	92	2	8	29	92	2	8	29	92	2	8	29	92
Lung (and bronchus)																		
Accumulation, administered substance, alveolus	1		0	0	0	0	0	0	0	0	3	0	0	0	0	0	0	0
	2		0	0	0	0	2	0	0	0	0	0	0	0	0	0	0	0
	3		0	0	0	0	1	0	0	0	0	0	0	0	0	0	0	0
Accumulation, administered substance, bronchus	1		0	0	0	0	2	0	0	0	0	0	0	0	0	0	0	0
	2		0	0	0	0	1	0	0	0	2	0	0	0	0	0	0	0
	3		0	0	0	0	0	0	0	0	1	0	0	0	0	0	0	0
Atelectasis, focal	1		0	0	0	0	1	0	0	0	2	0	0	0	0	0	0	0
	2		0	0	0	0	0	0	0	0	1	0	0	0	0	0	0	0
Cell infiltration, inflammatory, focal	1		0	0	0	0	0	0	0	0	0	0	0	0	2	0	2	3
	2		0	0	0	0	3	0	0	0	2	0	0	0	0	0	0	0
	3		0	0	0	0	0	0	0	0	1	0	0	0	0	0	0	0
Cell infiltration, macrophage, alveolus, focal	1		0	0	0	0	3	1	1	0	0	3	1	1	0	1	1	0
	2		0	0	0	0	0	2	2	3	0	0	0	0	0	0	0	3
Cell infiltration, macrophage, interstitium, focal	1		0	0	0	0	0	3	3	3	0	0	1	0	0	0	1	2
	2		0	0	0	0	0	0	0	0	0	3	1	3	0	0	0	0
Erosion, bronchus	1		0	0	0	0	0	0	0	0	2	0	0	0	0	0	0	0
Hyperplasia, lymphoid tissue	1		0	0	0	0	0	0	0	0	1	0	0	0	0	0	0	0
Hypertrophy, alveolar epithelium, focal	1		0	0	0	0	3	0	0	0	0	0	0	0	0	0	0	0
Hypertrophy, bronchial epithelium	1		0	0	0	0	3	1	0	0	2	1	0	0	0	0	0	0

Note: values indicate number of animals indicating lesion.
Grade: 1 = minimal, 2 = mild, 3 = moderate. Day: day of intratracheal instillation designated as Day 1.

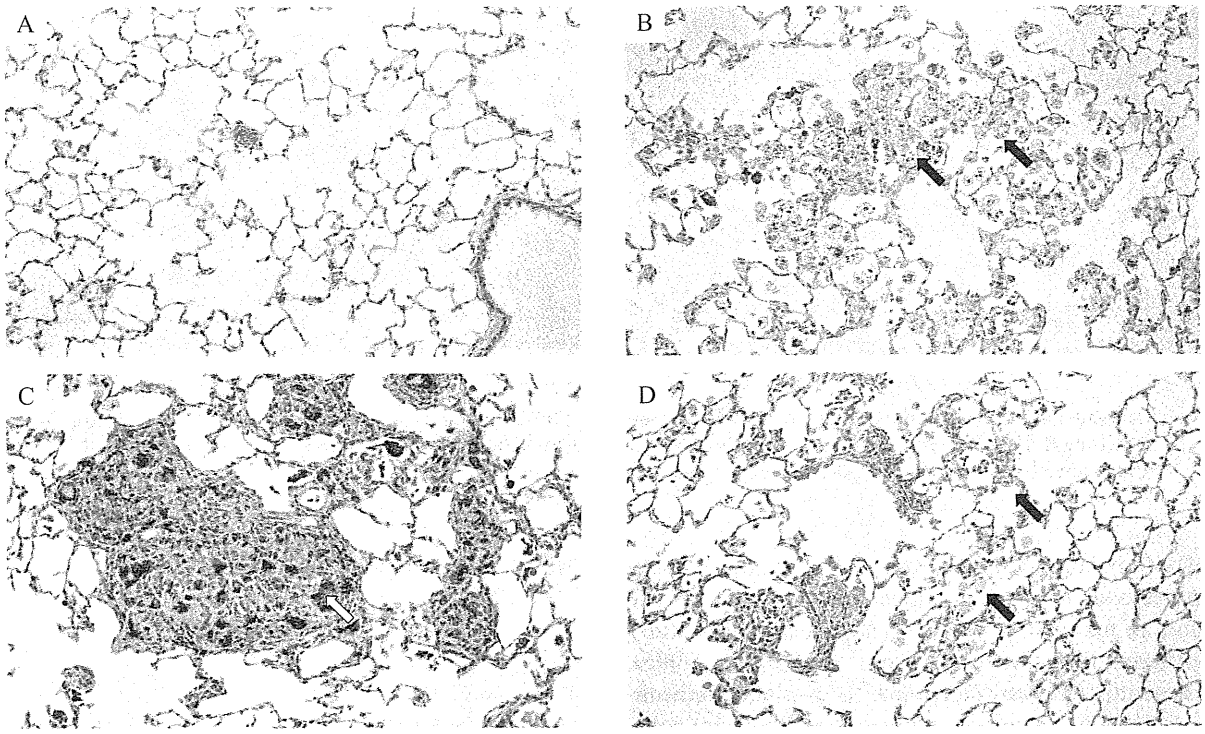

Fig. 7. Light microscopy of the lungs of rats exposed to non-ground and ground MWCNT, and corresponding controls on day 29. A) Control, no remarkable change. B) Ground MWCNT, foamy macrophage infiltration in alveolus. C) non-ground MWCNT, macrophage infiltration in interstitium. D) Min-U-Sil, foamy macrophage infiltration in alveolus.

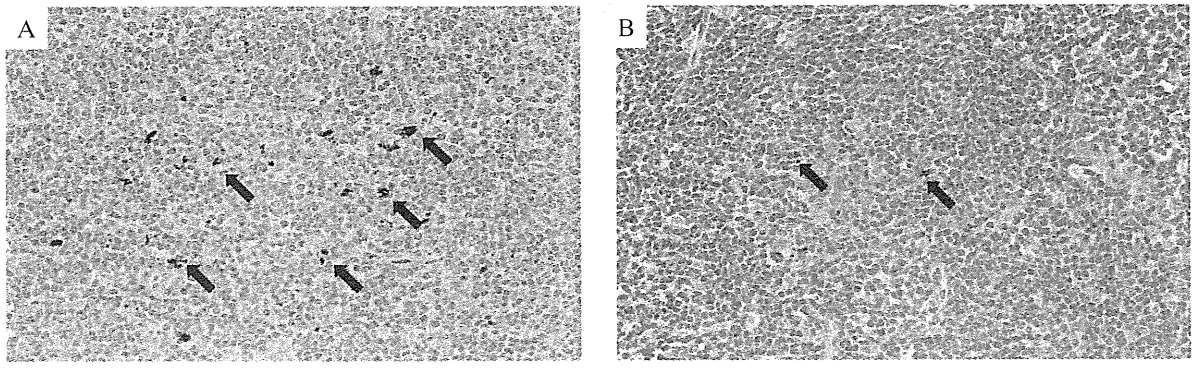

Fig. 8. Light microscopic view of bronchiolar lymph node of rats exposed to non-ground or ground MWCNT on day 29. A) Ground MWCNT: remarkable infiltration of macrophage including MWCNT without any inflammatory reactions than non-ground MWCNT. B) Non-ground MWCNT: infiltration of macrophage including MWCNT without any inflammatory reactions.

olar lymph nodes of rats given MWCNT. Since inflammatory change in the bronchiolar lymph nodes was observed in rats given Min-U-Sil, the biological activity on the discharge process of foreign body from the respiratory tract is considered to be remarkably different between MWCNT and Min-U-Sil.

It is estimated that the aerodynamic sizes of MWCNT become smaller than their original size, because MWCNT is widely used after the grinding process (Liu *et al.*, 2004). In fact, it is expected that MWCNT, which has

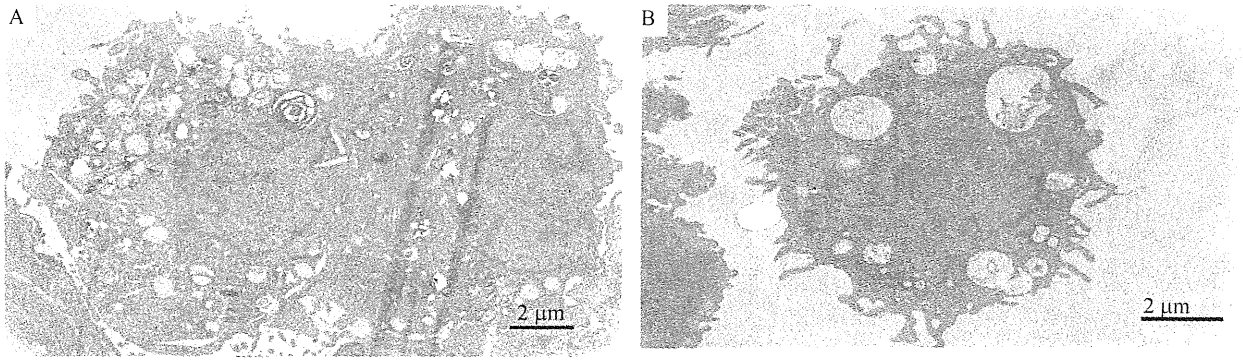

Fig. 9. Transmission electron microscopic view of macrophage in alveolus of rat exposed to non-ground or ground MWCNT. A) Ground MWCNT: macrophage in alveolus had lysosomes which developed remarkably. B) Non-ground MWCNT: macrophage in alveolus on day 29, there were no remarkable lysosomes.

small aerodynamic diameter due to the grinding, reaches deep into the lung in an occupational environment. The pulmonary toxicity of MWCNT obtained in this study was different from the recent report (Muller *et al.*, 2005). Consequently, it is considered that the available information on MWCNT induced pulmonary toxicity is not sufficient to evaluate the effects on human health. Since both of the above-mentioned studies did not have characterization data of the instilled suspensions, the pulmonary toxicity could not be compared between the studies. Therefore, the fibers in the suspensions must be characterized, at least for their length, diameter, and dispersion conditions in order to make a comparison with recent reports. Furthermore, the present study indicated that the different pulmonary toxicity occurred depending on the size of the particles in the suspension. These results suggested that the proper evaluation of the pulmonary toxicity of nanomaterial must include characterization of the instilled suspensions, even if it was only a single material.

There were no inflammatory reactions in the lung or bronchiolar lymph nodes in the rats given MWCNT 3 months after instillation. However, higher protein concentrations in BALF were observed in rats given MWCNT. Moreover, the long term effect of MWCNT on the lungs caused by grinding or non-grinding remained unclear in this study. These findings lead us to conclude that additional studies, such as examination of the fate of MWCNT in the lung and its long term effects on the lung are necessary.

ACKNOWLEDGMENT

This study was supported by Health Sciences Research Grants H18–kagaku-ippan-007 from the ministry of Health, Labor, and Welfare, Japan.

REFERENCES

Buford, M.C., Hamilton, R.F. and Holian, A. (2007): A comparison of dispersing media for various engineered carbon nanoparticles. Part. Fibre Toxicol., **4**, 6.

Donaldson, K., Aitken, R., Tran, L., Stone, V., Duffin, R., Forrest, G. and Alexander, A. (2006): Carbon nanotubes: A review of their properties in relation to pulmonary toxicology and workplace safety. Toxicol. Sci., **92**, 5-22.

Lam, C.W., James, J.T., McCluskey, R., Arepalli, S. and Hunter, R.L. (2006): A review of carbon nanotube toxicity and assessment of potential occupational and environmental health risks. Crit. Rev. Toxicol., **36**, 189-217.

Liu, C.H., Huang, H., Wu, Y. and Fan, S.S. (2004): Thermal conductivity improvement of silicone elastomer with carbon nanotube loading. Appl. Phys. Lett., **84**, 4248-4250.

Muller, J., Huaux, F., Moreau, N., Misson, P., Heilier, J., Delos, M., Arras, M., Fonseca, A., Nagy, J.B. and Lison, D. (2005): Respiratory toxicity of multi-wall carbon nanotubes. Toxicol. Appl. Pharmacol., **207**, 221-231.

Poland, C.A., Duffin, R., Kinloch, I., Maynard, A., Wallace, W.A.H., Seaton, A., Stone, V., Brown, S., Macnee, W. and Donaldson, K. (2008): Carbon nanotubes introduced into the abdominal cavity of mice show asbestos-like pathogenicity in a pilot study. Nat. Nanotechnol., **3**, 423-428.

Sager, T.M., Porter, D.W., Robinson, V.A., Lindsley, W.G., Schwegler-Berry, D.E. and Castranova, V. (2007): Improved method to disperse nanoparticles for *in vitro* and *in vivo* investigation of toxicity. Nanotoxicology, **1**, 118-129.

Takagi, A., Hirose, A., Nishimura, T., Fukumori, N., Ogata, A., Ohashi, N., Kitajima, S. and Kanno, J. (2008): Induction of mesothelioma in p53+/- mouse by intraperitoneal application of multi-wall carbon nanotube. J. Toxicol. Sci., **33**, 105-116.

The Journal of Toxicological Sciences (J. Toxicol. Sci.)
Vol.35, No.2, 265-270, 2010

Letter

Serum level of expressed in renal carcinoma (ERC)/ mesothelin in rats with mesothelial proliferative lesions induced by multi-wall carbon nanotube (MWCNT)

Yoshimitsu Sakamoto[1], Dai Nakae[1,2], Yoshiaki Hagiwara[3,4], Kanako Satoh[1], Norio Ohashi[1], Katsumi Fukamachi[5], Hiroyuki Tsuda[5], Akihiko Hirose[6], Tetsuji Nishimura[7], Okio Hino[3] and Akio Ogata[1]

[1]Department of Environmental Health and Toxicology, Tokyo Metropolitan Institute of Public Health, 3-24-1 Hyakunin'cho, Shin'juku-ku, Tokyo 169-0073, Japan
[2]Tokyo University of Agriculture, 1-1-1 Sakuragaoaka, Setagaya-ku, Tokyo, 156-8502, Japan
[3]Department of Pathology and Oncology, Juntendo University School of Medicine, 2-1-1 Hongo, Bunkyo-ku, Tokyo 113-8421, Japan
[4]Immuno-Biological Laboratory Co., Ltd., 1091-1 Naka, Fujioka, Gunma 375-0005, Japan
[5]Department of Molecular Toxicology, Nagoya City University, 1 Kawasumi, Mizuho-cho, Mizuho-ku, Nagoya, Aichi 467-8601, Japan
[6]Divisions of Risk Assessment, Biological Safety Research Center and [7]Environmental Chemistry, National Institute of Health Sciences, 1-18-1 Kamiyoga, Setagaya-ku, Tokyo 158-8501, Japan

(Received November 5, 2009; Accepted December 30, 2009)

ABSTRACT — Expressed in renal carcinoma (ERC)/mesothelin is a good biomarker for human mesothelioma and has been investigated for its mechanistic rationale during the mesothelioma development. Studies are thus ongoing in our laboratories to assess expression of ERC/mesothelin in sera and normal/proliferative/neoplastic mesothelial tissues of animals untreated or given potentially mesothelioma-inducible xenobiotics, by an enzyme-linked immunosorbent assay (ELISA) for N- and C-(terminal fragments of) ERC/mesothelin and immunohistochemistry for C-ERC/mesothelin. In the present paper, we intend to communicate our preliminary data, because this is the first report to show how and from what stage the ERC/mesothelin expression changes during the chemical induction of mesothelial proliferative/neoplatic lesions. Serum N-ERC/mesothelin levels were 51.4 ± 5.6 ng/ml in control male Fischer 344 rats, increased to 83.6 ± 11.2 ng/ml in rats given a single intrascrotal administration of 1 mg/kg body weight of multi-wall carbon nanotube (MWCNT) and bearing mesothelial hyperplasia 52 weeks thereafter, and further elevated to 180 ± 77 ng/ml in rats similarly treated and becoming moribund 40 weeks thereafter, or killed as scheduled at the end of week 52, bearing mesothelioma. While C-ERC/mesothelin was expressed in normal and hyperplastic mesothelia, the protein was detected only in epithelioid mesothelioma cells at the most superficial layer. It is thus suggested that ERC/mesothelin can be used as a biomarker of mesothelial proliferative lesions also in animals, and that the increase of levels may start from the early stage and be enhanced by the progression of the mesothelioma development.

Key words: Serum mesothelin, Rat, MWCNT, Mesothelial proliferative lesions

INTRODUCTION

Mesothelioma is a highly aggressive malignant tumor and developed in people previously exposed to asbestos, after a long latency period of 30-40 years. It is desired to establish a biomarker that can identify potential patients with early stage tumors or even as yet without tumors among the high-risk population.

Expressed in renal carcinoma (ERC)/mesothelin is a product of the *Erc* gene discovered in renal carcinomas of the Eker rats (Hino *et al.*, 1995) and confirmed as a homolog of the human *mesothelin/megakaryocyte poten-*

Correspondence: Yoshimitsu Sakamoto (E-mail: Yoshimitsu_Sakamoto@member.metro.tokyo.jp)

ciating factor gene (Hino, 2004; Yamashita *et al.*, 2000). A 71-kDa glycosylphosphatidylinositol anchor-type membranous protein is produced and physiologically cleaved by a furin-like protease to yield a membrane-binding 40-kDa C-terminal (C-ERC/mesothelin) and a secreting 31-kDa N-terminal (N-ERC/mesothelin) fragments (Chang and Pastan, 1996; Maeda and Hino, 2006; Yamaguchi, *et al.*, 1994). ERC/mesothelin is a useful marker for human mesothelioma cases (Hino *et al.*, 2007; Maeda and Hino, 2006) and its specific enzyme-linked immunosorbent assay (ELISA) system has been developed (Hagiwara *et al.*, 2008; Nakaishi *et al.*, 2007) for the clinical use (Maeda and Hino, 2006; Shiomi, *et al.*, 2006, 2008; Tajima *et al.*, 2008). The most important question is as to whether ERC/mesothelin can be efficient also in the early phase of the mesothelioma development, and studies are ongoing in our laboratories to assess ERC/mesothelin levels in animals untreated or given potentially mesothelioma-inducible xenobiotics.

We preliminarily assessed ERC/mesothelin levels using the samples of our previous study demonstrating the induction of mesothelial proliferative lesions in male Fisher 344 rats given multi-wall carbon nanotube (MWCNT) (Sakamoto *et al.*, 2009) In the present paper, we intend to communicate this preliminary data, despite its very limited sample numbers, because this is the first report to show how and from what stage the ERC/mesothelin expression changes during the chemical induction of mesothelial proliferative/neoplatic lesions.

MATERIALS AND METHODS

Ethical consideration of the experiments

An experimental protocol was approved by the Experiments Regulation/Animal Experiment Committees of the Tokyo Metropolitan Institute of Public Health for its scientific and ethical appropriateness, including concern for animal welfare, with strict obedience to domestically and internationally applicable declarations, laws, guidelines and rules.

Samples

Male Fisher 344 rats were purchased at their age of 4 weeks old from Charles River Laboratories Japan Inc. (Kanagawa, Japan) and maintained in our animal room (24-25°C, 50-60% relative humidity, 10 times/hr air ventilation and 12-hr light/dark cycle) until use.

Normal rat samples

Serum samples were obtained from 3, 1 and 2 untreated rats at their ages of 11, 42 and 81 weeks old, respectively.

Vehicle/MWCNT-treated rat samples

As detailed elsewhere (Sakamoto *et al.*, 2009), rats were given a single intrascrotal administration of 1 ml/kg body weight of vehicle (2% carboxymethylcellulose) or 1 mg/kg body weight of MWCNT at the age of 12 weeks old and left untreated for up to 52 weeks. In the present study, 9 samples were used: 3 from vehicle-treated rats killed as scheduled at the end of week 52, without any mesothelial changes; 3 from MWCNT-treated rats similarly killed, with mesothelial hyperplasias but without mesotheliomas; and 3 from other MWCNT-treated animals, 1 killed as moribund at week 40 and 2 killed as scheduled at the end of week 52, with early and advanced stages mesotheliomas and hemorrhagic ascites. Serum samples and in the last case an ascites sample were obtained at the time of the autopsy, and 10% neutrally buffered formalin-fixed, paraffin-embedded, mesothelial tissue samples were routinely prepared.

ERC/mesothelinin ELISA assay

Serum and ascites ERC/mesothelin levels were analyzed using rat N- and C-ERC/mesothelin assay kits (Immuno-Biological Laboratories [IBL] Co., Ltd., Gunma, Japan) adapting from the method of Hagiwara *et al.* (2008), the detection limit being 0.1 ng/ml. A 6-μl aliquot was diluted with 234 μl of phosphate-buffered saline containing 1% bovine serum albumin and 0.05% Tween 20. Assays were conducted according to the manufacturer' instruction to measure an optical density at 450 nm. Each sample was assessed in duplicate.

Histology and C-ERC/mesothelin immunohistochemistry

Two serial, 4-μm-thick sections were prepared and deparaffinized. One was processed through a routine hematoxylin and eosin (HE) staining procedure and histgtologically examined. The other was heated in 10 mM citrate buffer, pH 6.0, treated with 3% hydrogen peroxide, incubated with a primary anti-rat C-ERC/mesothelin antibody (IBL) overnight at 4°C, washed with tris-buffered saline, and re-incubated using an Envision system (DAKO Japan Company, Limited, Tokyo, Japan). Signals were visualized by 3,3'-diaminobenzidine, and the sections were counter-stained with hematoxylin.

Statistical analysis

Statistical significance of intergroup difference for the N-ERC/mesothelin level was assessed using Student's *t*-test, and *p*-values less than 0.05 were considered significant.

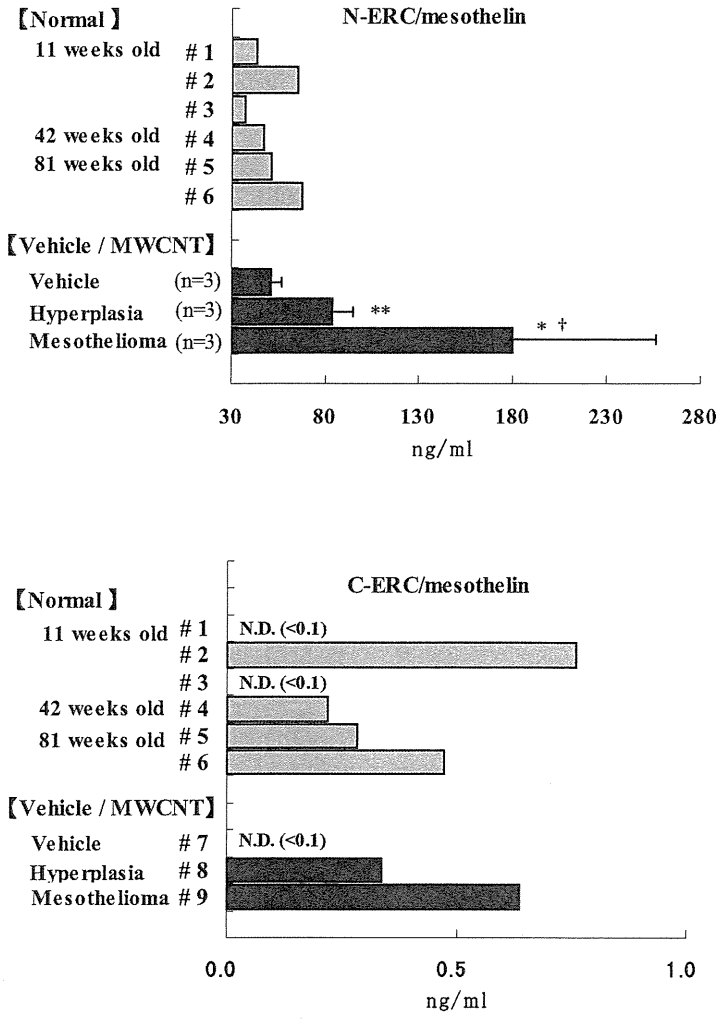

Fig. 1. Serum levels of A, N-ERC/mesothelin and B, C-ERC/mesothelin. Each data is a mean of duplicate assays. #1- #6 in Fig. A and #1- #9 in Fig. B show sample numbers. "N.D.", not detectable, indicates that the data was below the detection limit of 0.10 ng/ml. Values of N-ERC/mesothelin of samples from vehicle, hyperplasia and mesothelioma groups in Fig. B represent the means ± S.D. (n = 3).
Statistical significant difference by Student's t-test: $^{*}P < 0.05$, $^{**}P < 0.01$ as compared from the vehicle group and $^{\dagger}P < 0.05$ as compared from the hyperplastic group.

RESULTS AND DISCUSSION

Serum N-ERC/mesothelin levels of the normal rats were 43.4, 65.1 and 37.3 ng/ml, 47.1 ng/ml and 51.1 and 67.5 ng/ml; while those of C-ERC/mesothelin were < 0.1, 0.8 and < 0.1 ng/ml, 0.2 ng/ml and 0.3 and 0.5 ng/ml; for 11, 42 and 81 weeks of their ages, respectively (Fig. 1). These were respectively within the same range, and the N-ERC/mesothelin levels were substantially higher than the C-ERC/mesothelin levels. No apparent age-dependent changes were obtained for either fragment.

Serum N-(n = 3) and C-(n = 3) ERC/mesothelin levels of the vehicle-treated rat was 51.4 ± 5.6 ng/ml and < 0.1 ng/ml, respectively, within the normal ranges, whereas serum N-ERC/mesothelin levels of MWCNT-treated rats were increased by the induction of mesothelial hyperpla-

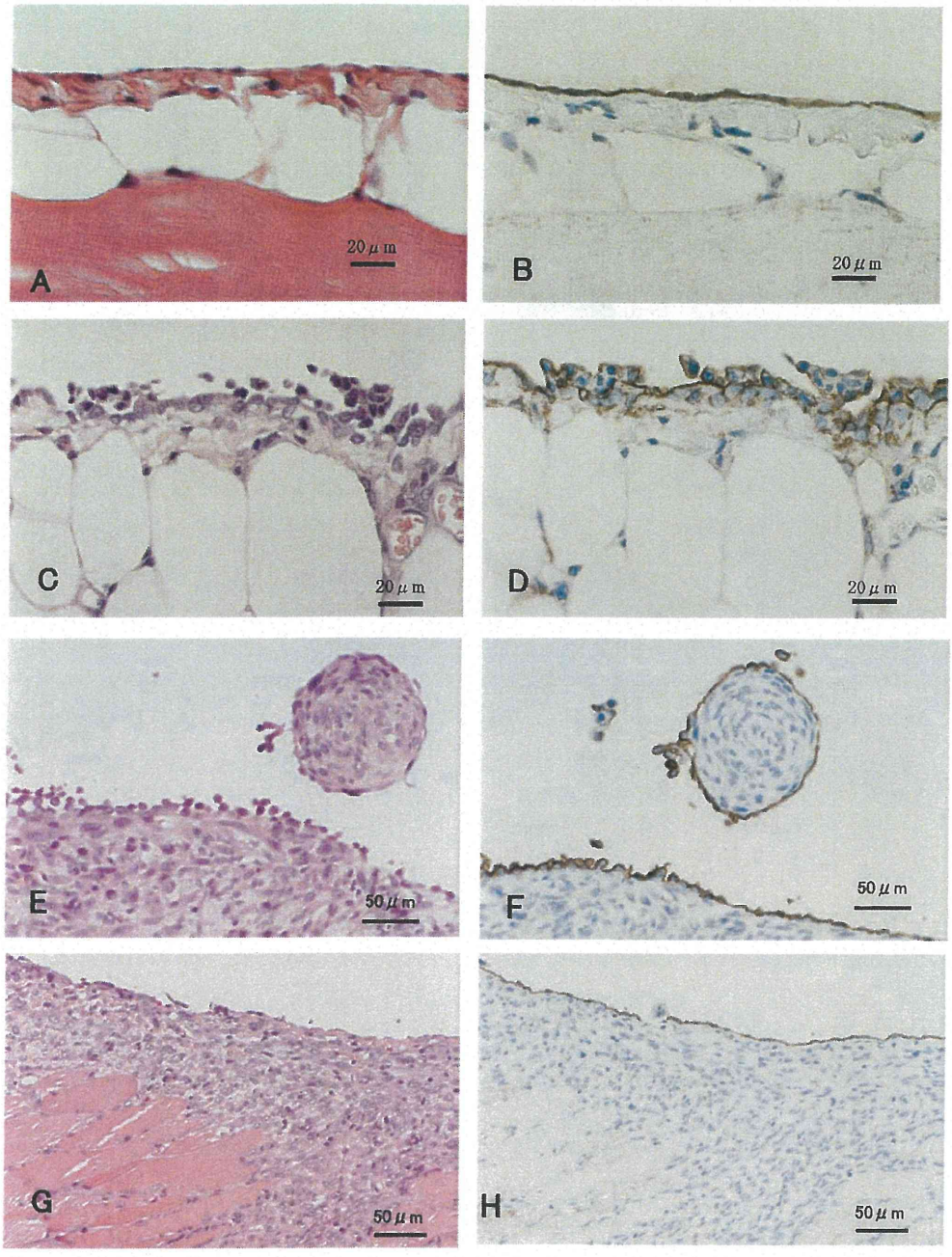

Fig. 2. Representative histology and C-ERC/mesothelin immunohistochemistry.
A, intact mesothelia in the parietal peritoneum of the vehicle-treated rat, HE; B, A's serial section, C-ERC/mesothelin; C, a mesothelial hyperplasia in the retroperotineal fat tissue of the MWCNT-treated rat, HE; D, C's serial section, C-ERC/mesothelin; E, an early-stage epithelioid/polypoid type mesothelioma in retroperotineal fat tissue of the other MWCNT-treated rat, HE; F, E's serial section, C-ERC/mesothelin; G, an advanced-stage mostly-sarcomatoid/invasive-nodular type mesothelioma in the diaphragm of the MWCNT-treated rat (the same animal as E/F), HE; H, G's serial section, C-ERC/mesothelin. Bars with their lengths are inserted to indicate magnifications.

sia (83.6 ± 11.2 ng/ml) and further by that of mesothelioma (179 ± 77 ng/ml; 3,004 ± 665 ng/ml in ascites) (Fig. 1). Serum N-ERC/mesothelin levels in experimental animals have only been assessed in Eker and Wistar rats and nude mice, untreated or transplanted with a rat mesothelioma cell line, MetEt-40 (Hagiwara *et al.*, 2008; Nakaishi *et al.*, 2007). The present data for the first time demonstrates that serum N-ERC/mesothelin level was increased already at the stage of preneoplastic, mesothelial hyperplasia and further increased by the chemical induction of mesothelioma. This may be in line with the recent findings that elevated serum mesothelin is detected before the development of grossly visible carcinoma lesions in a rat pancreatic carcinoma models (Fukamachi *et al.*, 2009). In human mesothelioma, it has been reported that N-ERC/mesothelin level increased with the stage went up of epithelioide type mesothelioma in human case (Shiomi *et al.*, 2008). It is not known, however, how N-ERC/mesothelin levels change in the stage of preneoplasia at this moment. Large-scaled, detailed investigations using the MWCNT-mesothelioma model are ongoing in our laboratories.

Serum C-ERC/mesothelin levels of MWCNT-treated rats were 0.4 and 0.6 ng/ml, within the normal/vehicle range (Fig. 1B). This is in accordance with the previous finding in nude mice transplanted with MetET-40 (Hagiwara *et al.*, 2008), and can be attributed to the membrane-binding property of C-ERC/mesothelin (Maeda and Hino, 2006). Ascites level of C-ERC/mesothelin in the mesothelioma case was slightly increased to 10.9 ng/ml (Fig. 1B). This is speculated to result from a release of C-ERC/mesothelin by phosphatidylinositol-specific phospholipase C (Chang and Pastan, 1996) or a contamination of desquamated mesothelioma cells.

Immuohistochemical C-ERC/mesothelin signals were constantly detected in cell membranes. C-ERC/mesothelin was detected in intact (Figs. 2A and B) and hyperpastic (Figs. 2C and D) mesothelia. Taken the ELISA data together, it might be possible that the ERC/mesothelin level starts increased from the preneoplastic stage.

C-ERC/mesothelin was found only in epithelioid (mesothelioid) tumor cells present at the most superficial layer of early-stage, epithelioid/polypoid (Figs. 2E and F) and advanced-stage, mostly-sarcomatoid/invasive-nodular (Figs. 2G and H) types of mesotheliomas. In humans, epithelioid types, but not sarcomatoid types or sarcomatoid components of biphasic (mixed) types, immunohistochemically express C-ERC/mesothelin (Chang and Pastan, 1996; Shiomi *et al.*, 2008; Ordóñez, 2003). Accordingly, serum N-ERC/mesothelin levels were only slightly increased or often unchanged in sarcomatoid and biphasic types, in contrast to the epithelioid type (Hassan *et al.*, 2006; Shiomi *et al.*, 2008). The present findings suggest that the increaseof ERC/mesothelin levels in mesotheliomas may be a universal event for all types and stages, and that C-terminal fragments may become unproduced or changed its tertiary structure and/or epitope construction by the neoplastic conversion.

In conclusion, the present data suggests that ERC/mesothelin can be used as a biomarker of mesothelial proliferative lesions also in animals, and that its increase of its levels may start from the early stage and be enhanced by the progression of the mesothelioma development.

ACKNOWLEDGMENTS

This work was supported in part by a research budget of the Tokyo Metropolitan Government, Japan, and Grants-in-Aid for Scientific Research from the Ministry of Health, Labour and Welfare of Japan, from the Japan Society for the Promotion of Science, and from the Ministry of Education, Culture, Sports, Science and Technology of Japan. This study was also partially supported by a consignment expense for Molecular Imaging Program on "Research Base for PET Diagnosis" from the Ministry of Education, Culture, Sports, Science and Technology of Japan.

REFERENCES

Chang, K. and Pastan, I. (1996): Molecular cloning of mesothelin, a differentiation antigen present on mesothelium, mesotheliomas, and ovarian cancers. PNAS USA, **93**, 136-140.

Fukamachi, K., Tanaka, H., Hagiwara, Y., Ohara, H., Joh, T., Iigo, M., Alexander, D.B., Xu, J., Long, N., Takigahira, M., Yanagihara, K., Hino, O., Saito, I. and Tsuda, H. (2009): An animal model of preclinical diagnosis of pancreatic ductal carcinomas. Biochem. Biophys. Res. Commun., **390**, 636-641.

Hagiwara, Y., Hamada, Y., Kuwahara, M., Maeda, M., Segawa, T., Ishikawa, K. and Hino, O. (2008): Establishment of a novel specific ELISA system for rat N- and C-ERC/mesothelin. Rat ERC/mesothelin in the body fluids of mice bearing mesothelioma. Cancer Sci., **99**, 666-670.

Hassan, R., Remaley, A.T., Sampson, M.L. Zhang, J., Cox, D.D., Pingpank, J., Alexander, R., Willingham, M., Pastan, I. and Onda, M. (2006): Detection and quantitation of serum mesothelin, a tumor marker for patients with mesothelioma and ovarian cancer. Clin. Cancer Res., **12**, 447-453.

Hino, O., Kobayashi, E., Nishizawa, M., Kubo, Y., Kobayashi, T., Hirayama, Y., Takai, S., Kikuchi, Y., Tsuchiya, H., Orimoto, K., Kajino, K., Takahata, T. and Hitani, H. (1995): Renal carcinogenesis in the Eker rat. J. Cancer Res. Clin. Oncol., **121**, 602-605.

Hino, O. (2004): Multistep renal carcinogenesis in the Eker (*Tsc2* gene mutant) rat model. Curr. Mol. Med., **4**, 807-811.

Hino, O., Shiomi, K. and Maeda, M. (2007): Diagnostic biomarker of asbestos-related mesothelioma: example of translational research. Cancer Sci., **98**, 1147-1151.